Limit cycles and their stability in a passive bipedal gait

Ambarish Goswami Bernard Espiau Ahmed Keramane

INRIA Rhône-Alpes
46 Avenue Félix Viallet
38031 Grenoble Cedex 1, France
Ambarish.Goswami@inria.fr

Abstract

It is well-known that a suitably designed unpowered mechanical biped robot can "walk" down an inclined plane with a steady gait. The characteristics of the gait (e.g., velocity, time period, step length) depend on the geometry and the inertial properties of the robot and the slope of the plane.

A passive motion has the distinction of being "natural" and is likely to enjoy energy optimality. Investigation of such motions may potentially lead us to strategies useful for controlling active walking machines.

In this paper we demonstrate that the nonlinear dynamics of a simple passive "compass gait" biped robot can exhibit periodic and stable limit cycle. Kinematically the robot is identical to a double pendulum (or its variations such as the Acrobot and the Pendubot). Simulation results also reveal the existence of a stable gait with unequal step lengths. We also present an active control scheme which enlarges the basin of attraction of the passive limit cycle.

1 Introduction

One of the most sophisticated forms of legged motion is that of biped locomotion. From a dynamic systems point of view, human locomotion stands out among other forms of biped locomotion chiefly due to the fact that during a significant part of the human walking cycle the moving body is not in the static equilibrium.

At the INRIA Laboratory in Grenoble, France, we have started working on the development of an anthropomorphic biped walker. The envisioned prototype will have elementary adaptation capability on an unforeseen uneven terrain. The purpose of the project is not limited to the realization of a complex machine, the construction and control of which nevertheless pose formidable engineering challenge. We also intend to initiate a synergy between robotics and human gait study. Human locomotion, despite being well studied and enjoying a rich database, is not well understood and a robotic simulcrum potentially can be very useful.

In order to gain a better understanding of the inherently non-linear dynamics of a full-fledged walking machine we have found it instructive to first explore the behavior of a particularly simple walker model. Inspired by the research of [1] and [4], and the relatively more recent research on passive walking machines [11] we have considered the model of a so-called "compass gait" walker. Based on the same kinematics as that of a double pendulum, our compass gait model has the Acrobot [2] [14] and the Pendubot [3] as its nearest cousins.

McGeer[11] designed, among other prototypes, a simple knee-less biped robot and studied its gravity-induced passive motion on an inclined plane. He demonstrated that the prototype can attain a stable periodic motion and analyzed this behavior with a linearized mathematical model. In order to maintain a stable uniform locomotion, the joint variables (displacement, velocity) of the robot must follow a steady cyclic trajectory. Our objective here is to study such a passive system by means of its full non-linear equations and using tools available for non-linear systems analysis.

Related to this somewhat local objective there are several long term motivations which are all connected to the eventual goal of obtaining a simple biologically-inspired adaptive control law for our future prototype. The first is our intuitive support of the conjecture that legged locomotion and possibly all inter-limb coordinations are identified by non-linear limit cycle oscillatory processes [10]. Next, a passive motion is attractive because it is *natural* and it does not require any external energy source. If an active control law closely mimics a passive system it is likely to enjoy certain inherent advantages of the passive system such as the energy optimality, periodicity, and stability. Of particular in-

terest in this respect is the hypothesis that a great part of the swing stage in human locomotion is passive, a hypothesis that is supported by many studies.

Simulation studies of our passive compass gait walker show that such cyclic motions are represented by stable limit cycles in the phase space of the robot. We have also shown the existence of stable but unsymmetric compass gait where two successive step lengths are unequal. Finally we use a passivity-mimicking control law that significantly enhances the stability robustness of the walker.

2 The compass gait model

2.1 The kinematics

We consider a very simple model of a biped robot as shown in Figure 1. In this figure, m is the lumped mass of each leg and m_H is the hip mass. The leg-length is denoted as l which is divided into a and b, where a is the distance from the leg-tip to the position of m and b is the distance from m to the hip center. θ_s and θ_{ns} are the angles made by the biped legs with the vertical (counterclockwise positive). The total angle between the legs, which we call the "inter-leg angle" is 2α when both legs are touching the ground. The slope of the ground is denoted by the angle ϕ.

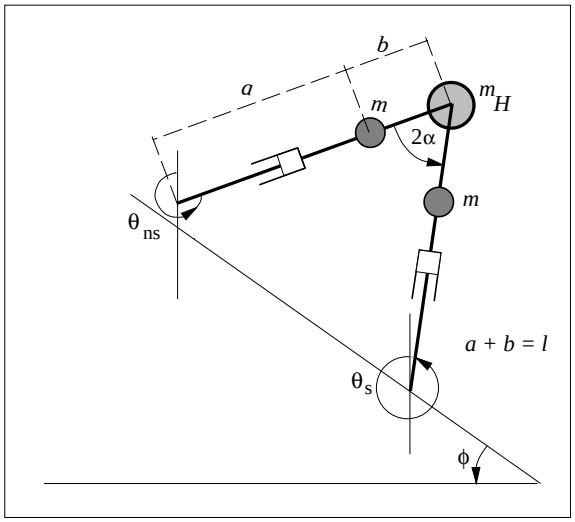

Figure 1: Model of a Compass Gait Biped Robot on a Slope

All masses in our model are considered point-masses. The legs are identical with each leg having a telescopically retractable knee-joint with a massless lower leg (shank). This solves the problem of foot clearance without affecting robot dynamics. The gait consists of a single-support or swing stage and an instantaneous transition stage. During the swing stage the robot behaves exactly like an inverted planar double pendulum. During the transition stage the support is transferred from one leg to the other. The robot is assumed to move on a plane surface, horizontal or inclined. The impact of the swing leg with ground is assumed to be frictional inelastic. The friction is sufficient to ensure that no slip occurs between the ground and the foot.

The telescopic retraction of the leg solves the problem of foot clearance without affecting robot dynamics. Our emphasis here is more on the simplicity of the model than its physical realizability. We should also point out that the simplifying assumptions made above are routinely made in the biped robot literature and are not unique for this work.

2.2 The governing equations

2.2.1 Dynamics of the single support stage

As implied in the assumptions above, the biped is *always* in the single support stage except when the support is instantaneously transferred from one foot to the other. The dynamic equations for this single support stage are rather well-known (see for instance, [12]). Since the legs of the robot are assumed identical, the equations are similar regardless of the support leg considered. The equations have the following form:

$$\boldsymbol{M}(\boldsymbol{\theta})\ddot{\boldsymbol{\theta}} + \boldsymbol{N}(\boldsymbol{\theta},\dot{\boldsymbol{\theta}})\dot{\boldsymbol{\theta}} + \boldsymbol{G}(\boldsymbol{\theta}) \;=\; \boldsymbol{S}\boldsymbol{u} \qquad (1)$$

where $\boldsymbol{M}(\boldsymbol{\theta})$ is the 2×2 inertia matrix, $\boldsymbol{N}(\boldsymbol{\theta},\dot{\boldsymbol{\theta}})$ is a 2×2 matrix with the centrifugal coefficients, $\boldsymbol{G}(\boldsymbol{\theta})$ is a 2×1 vector of gravitational torques and $\boldsymbol{S}$ is a 2×3 matrix which selects the actuator torques. Also, $\boldsymbol{\theta} = [\theta_{ns} \;\; \theta_s]^T$ is the vector of joint angles (see Figure 1) and $\boldsymbol{u} = [u_{ns} \;\; u_H \;\; u_s]^T$ is the vector of joint torques. The subscripts ns, H, and s denote the non-support foot, hip, and the support foot, respectively. For the most part of this paper we deal with a passive model where $\boldsymbol{u} = \boldsymbol{0}$. The parameters used for our simulations are $a = b = 0.5m$, $l = a + b$, $m_H = 2m = 10kg$.

The 4-component state vector for the robot is $\boldsymbol{x} = [\theta_{ns} \;\; \theta_s \;\; \dot{\theta_{ns}} \;\; \dot{\theta_s}]^T$. Thus we have $\dot{\boldsymbol{x}_1} = \boldsymbol{x}_3$, $\dot{\boldsymbol{x}_2} = \boldsymbol{x}_4$ and the time derivatives of $\boldsymbol{x}_3$ and $\boldsymbol{x}_4$ are obtained by rearranging Equations 1 as $[\dot{\boldsymbol{x}_3} \;\; \dot{\boldsymbol{x}_4}]^T = \boldsymbol{M}^{-1}(\boldsymbol{S}\boldsymbol{u} - \boldsymbol{N}\dot{\boldsymbol{\theta}} - \boldsymbol{G})$.

2.2.2 Transition equations

Ideally, during transition, two things happen simultaneously: the swing leg touches the ground and the support leg leaves the ground. For an inelastic no-sliding

collision of the robot foot with the ground the robot's angular momentum during the collision is conserved [8]. This allows us to linearly relate the post-impact and the pre-impact angular velocities of the robot in the following way:

$$\dot{\boldsymbol{\theta}}(T+\varepsilon) \quad = \quad \boldsymbol{H}(\boldsymbol{\theta}(T))\dot{\boldsymbol{\theta}}(T-\varepsilon). \qquad (2)$$

$\dot{\boldsymbol{\theta}}(T-\varepsilon)$ and $\dot{\boldsymbol{\theta}}(T+\varepsilon)$ are the angular velocities just before and after the transition, which takes place at time $t = T$, and ε is a small time interval. Although, for simplicity, transition is assumed to be instantaneous, we should remember that in the actual physical system the hind leg may leave the ground and start swinging *only after* the front leg has hit the ground. $\boldsymbol{H}(\boldsymbol{\theta}(T))$ is a 2×2 matrix. At the double support stage, the inter-leg angle 2α fully defines the biped geometry. In other words, $\boldsymbol{H}$ is a function of α only.

The transition equations are derived from the equations $\boldsymbol{Q}(\alpha)\dot{\boldsymbol{\theta}}(T+\varepsilon) = \boldsymbol{P}(\alpha)\dot{\boldsymbol{\theta}}(T-\varepsilon)$ whose left hand side and the right hand side are respectively the angular momentum of the robot after and before the impact with the ground. Comparing this equation with the Equation 2 we can write $\boldsymbol{H}(\alpha) = \boldsymbol{Q}(\alpha)^{-1}\boldsymbol{P}(\alpha)$.

We also have during the transfer:

$$\theta_{ns}(T) + \theta_s(T) \quad = \quad -2\phi \qquad (3)$$

$$\text{and } 2\alpha(T) \quad = \quad \pm(\theta_s(T) - \theta_{ns}(T)) \qquad (4)$$

where $+$ and $-$ correspond to the instants just after and just before the change of support, respectively.

3 Description of a typical limit cycle

Let us continue our discussion of the system dynamics, the existence of limit cycles, and their stability with the help of a phase portrait of the robot. As the actual phase space of the robot is four dimensional and is not possible to visualize graphically, we present here the phase portrait of one leg. In Figure 2 we show the angular displacement/angular velocity behavior of one single leg of the robot as it alternately becomes the support leg and the swing leg. The figure shows a cyclic phase trajectory obtained after the robot has walked long enough such that the initial transients have died down.

In Figure 2 we may start following the phase trajectory at instant marked I in the figure, corresponding to time $t = \varepsilon$, when the rear leg just loses contact with the ground (i.e., it becomes the swing leg). Just before, the front leg touched the ground (i.e., it became the support leg). The corresponding stick diagram shows a black circle on the front foot to imply ground contact. The phase trajectory evolves in the clockwise sense in this diagram as shown by the arrowheads. While crossing the velocity axis (at a positive velocity), the biped is in the vertical configuration. Instant II corresponds to time $t = T - \varepsilon$ when the swing leg is about to touch the ground. The impact between the swing foot and the ground occurs at time $t = T$. At a slightly later time, marked as instant III, the other foot starts its swing and subsequently executes the lower half of the phase plane. The velocity jump of the current leg (the non-support leg of instant I) observed between the instant IV and the instant I is due to the impact of the other leg with the ground.

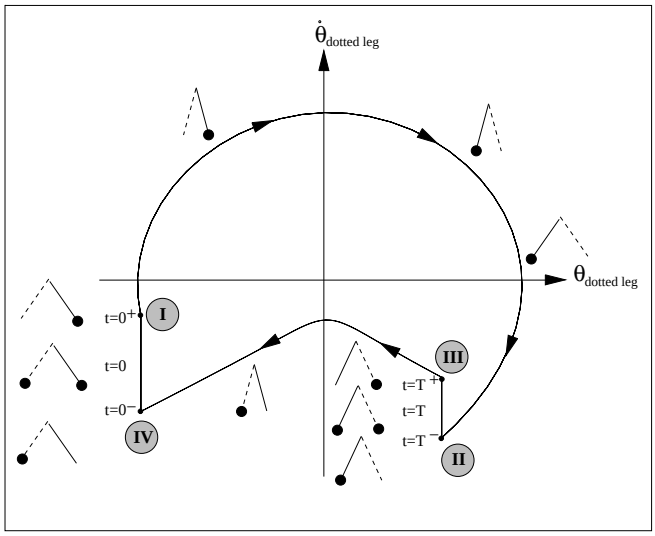

Figure 2: Phase Portrait of a Periodic Walk. This figure corresponds to only one of the joint variables of the biped. One cycle in the figure corresponds to two steps of the robot. On the outside of the cyclic portrait, the configuration of the biped has been shown with small stick diagrams. In these diagrams, one leg is dotted, the other leg is solid, and a black circle at the foot indicates the supporting leg.

Figure 2 represents a 2D projection of the complete 4D phase space. A projection of the phase space does not necessarily preserve the properties of the complete phase portrait of a system. For example, we often encounter phase trajectories crossing each other in our reduced phase diagram which is an impossibility in the full phase space. Also the adjacency of two trajectories in our reduced phase space does not necessarily imply their adjacency in the actual phase space; trajectories of equal length at two different parts of the diagrams do not necessarily imply their equality. Some features are, however, preserved in the projection of a phase space, a very useful one being that the cycles in the full

phase space are also cycles (possibly self-intersecting) in its projections.

4 The equilibrium of potential and kinetic energies

As shown in Figure 2 a passive compass biped, when started with favorable initial conditions, may walk down an inclined plane in a steady cyclic gait. We associate this to a limit cycle behavior of the piecewise continuous non-linear system represented by Equations 1 and 2.

Typically, the existence of a limit cycle in a dynamical system is associated with a contraction of the phase space volume as the system evolves in time. The presence of dissipative elements in the system cause a phase space volume contraction and favors (but does not guarantee) the existence of a limit cycle. Noting that our robot has a phase space volume conserving Hamiltonian dynamics during the swing stage we naturally search for the cause of the existence of limit cycle. The answer lies in the impact equations (Eq. 2). In fact, the robot mechanism behaves similar to that of a mechanical clock. In a clock the energy loss due to friction during a cycle is exactly compensated by an energy "kick" at definite intervals. For the robot the kinetic energy (KE) gain due to the conversion of the gravitational potential energy (PE) in a step is absorbed in an instantaneous impact at the touchdown.

Once we have found a limit cycle we may characterize it with several parameters. A limit cycle for slope $\phi = 3^\circ$ can be characterized by its step length (0.5354m), step period (0.734sec) and the total mechanical energy (153.078J). It is interesting that we have so far been unable to find two distinct stable limit cycles for the same ground slope. If this is true, this would indicate some underlying organizing principle which completely determines the dynamics of the robot once the ground slope is specified.

Significant amount of insight may be gained from a KE vs. PE plot of the robot (see Figure 3). In the swing stage of the robot KE + PE is constant and the energy trajectory (line BC) is a straight line making a 135° angle with the KE axis. The trajectory of the robot, starting from point A follows ABAC. Point C is the touchdown point where an impact occurs with the ground. The instantaneous loss of KE is shown by the line CD in the diagram. Total loss of PE in one step is given by the distance CF. For a periodic gait therefore, CF = CD.

For a steady state motion on a plane of known inclination, we can calculate the amount of PE lost in each step. For a passive biped executing a symmetric gait (in which the two legs are indistinguishable), we can consider only one half of the cycle shown in Figure 2. At stage III the joint positions and joint variables "initialize" themselves except that the legs are now interchanged. If the robot executes a periodic motion, the energy of the system should return to its initial value after every cycle. For a symmetric gait, the KE and the PE of the system should also initialize themselves after every half cycle.

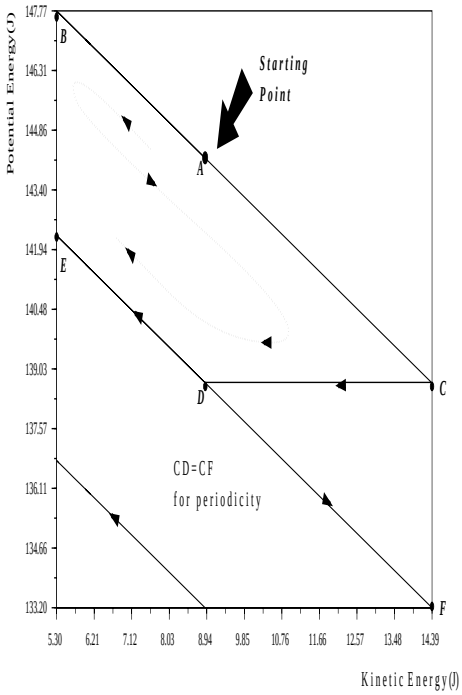

Figure 3: The KE vs. PE Diagram of a Compass Gait. For a steady periodic gait CD = CF.

Using these conditions we find the following equation which is in terms of two variables corresponding to the initial velocities of the two legs of the robot.

$$\dot{\boldsymbol{\theta}}_I^T \boldsymbol{J}^T ((\boldsymbol{H})^{-1^T} \boldsymbol{M}_{II} \boldsymbol{H}^{-1} - \boldsymbol{M}_{II}) \boldsymbol{J} \dot{\boldsymbol{\theta}}_I = 8mgLsin\phi. \tag{5}$$

where $\boldsymbol{J}$ is a 2×2 skew-symmetric matrix with unity off-diagonal elements meant to interchange support and non-support leg variables, L is the step length and other parameters have their usual meaning.

If we somehow determine one of the velocities, the other velocity may be calculated with the above equation. This equation does not help us in searching for a limit cycle but rather checks the validity of a cycle once it has been identified. The information that we used in obtaining the equation is based on energy alone and does not involve the dynamics of the system in between two touchdowns.

5 Local stability of the limit cycle

The concept of gait stability as applied to a walking machine is hard to define but is crucial for the performance analysis of the systems. The conventional definitions of stability of a system around an equilibrium point are not immediately suitable for such system. We follow Hayashi [7] in defining the stability of the system in terms of its *orbital stability*.

Let us first consider a continuous nonlinear system of the general form $\dot{\boldsymbol{x}} = \boldsymbol{f}(\boldsymbol{x}, t)$ from which we may eliminate time t and express the solution as a trajectory in the vector space of the states $\boldsymbol{x}$. In this reduced space one may imagine time to be the velocity associated with the representative point along the trajectory. The phase trajectory C of this system is orbitally stable if, given $\varepsilon > 0$, there is $\delta > 0$ such that, if R' is a representative point (on another trajectory C') which is within a distance δ of C at time t_0, then R' remains within a distance ε of C for $t \geq 0$. If no such δ exists, C is orbitally unstable. Analogous to the asymptotic stability of the conventional definition we may say that if the trajectory C is orbitally stable and, in addition, the distance between R' and C tends to zero as time goes to infinity, the trajectory C is asymptotically orbitally stable.

Notice that orbital stability requires that the trajectories C and C' remain near each other, whereas stability of the solution $\boldsymbol{x}(t)$ requires that, in addition, the representative points R and R' (on C and C' respectively) should remain close to each other, if they were close to each other initially.

The effect of a stable limit cycle in the phase plane will be to attract and absorb the nearby phase trajectories. A system starting from a state on the limit cycle will continue to travel on it. A surrounding area, called the domain or the basin of attraction of the limit cycle, is the region in which this attracting feature is valid. It is interesting to note here that the whole phase plane can be the domain of a Van der Pol oscillator, for a certain selection of its parameters. This property was utilized in an innovative control scheme of a biped robot [9].

One way to investigate the local stability of a limit cycle is to slightly perturb the states from the limit cycle and to observe the first return map of Poincaré. As a natural choice of the Poincaré section we take the condition that the swing leg of the robot touches the ground. For two successive touchdowns of the same leg the states of the robot can be related as

$$\boldsymbol{x_k} = F(\boldsymbol{x_{k-1}}) \tag{6}$$

For a cyclic phase trajectory the first return map is a point $\boldsymbol{x}^*$, called the *fixed point* of the mapping [6]. On a cyclic trajectory, therefore, $\boldsymbol{x_k} = \boldsymbol{x_{k-1}}$ and we can write, $\boldsymbol{x}^* = F(\boldsymbol{x}^*)$. For a small perturbation $\Delta\boldsymbol{x}^*$ around the limit cycle the nonlinear mapping function F can be expressed in terms of Taylor series expansion as

$$F(\boldsymbol{x}^* + \Delta\boldsymbol{x}^*) \approx F(\boldsymbol{x}^*) + (\nabla F)\Delta\boldsymbol{x}^* \tag{7}$$

where ∇F is the gradient of F with respect to the states. Since $\boldsymbol{x}^*$ is a cyclic solution, we can rewrite Equation 7 as

$$F(\boldsymbol{x}^* + \Delta\boldsymbol{x}^*) \approx \boldsymbol{x}^* + (\nabla F)\Delta\boldsymbol{x}^* \tag{8}$$

The mapping F is stable if the first return map of a perturbed state is closer to the fixed point. This property can be viewed as the contraction of the phase space around the limit cycle. Mathematically this means that the magnitude of the eigenvalues of ∇F at the fixed point $\boldsymbol{x}^*$ is strictly less than one. From Equation 8 we write $(\nabla F)\Delta\boldsymbol{x}^* \approx F(\boldsymbol{x}^* + \Delta\boldsymbol{x}^*) - \boldsymbol{x}^*$ where $F(\boldsymbol{x}^* + \Delta\boldsymbol{x}^*)$ is the first return map of the perturbed state $\boldsymbol{x}^* + \Delta\boldsymbol{x}^*$. As it is not practical to analytically calculate the matrix (∇F) we do so numerically. One straightforward method is to perturb one state at a time by a small amount and observe its first return map. Repeating this procedure once for each state we obtain an equation of the form

$$(\nabla F)\boldsymbol{\tau} = \boldsymbol{\mu} \tag{9}$$

where the 4×4 diagonal matrix $\boldsymbol{\tau}$ contains as its diagonal entries the perturbations of the state variables $(\Delta {x_i}^*)$. The i^{th} column of the 4×4 matrix $\boldsymbol{\mu}$ gives in terms of the four states how far away from the periodic solution the first return map shows up due to a perturbation of the i^{th} state variable. Assuming that $\boldsymbol{\tau}$ is non-singular, computation of ∇F is straightforward: $\nabla F = \boldsymbol{\mu}\boldsymbol{\tau}^{-1}$.

In one simulation with a 3° slope we compute the eigenvalues of ∇F to be $-0.252 + 0.215i$, $-0.252 - 0.215i$, 2.55×10^{-9}, and 0.014. The corresponding absolute values are 0.331, 0.331, 2.55×10^{-9}, and 0.014. Thus the cycle is stable. We note here that by the mere fact that we have found a limit cycle by means of numerical simulation practically guarantees that the cycle is stable. Unless we *accidentally* hit the exact states on a limit cycle unstable limit cycles are never visible in numerical trials.

For the given cycle, there is a zero eigenvalue. This is expected ([13]). The existence of this eigenvalue can be interpreted as that the perturbation has been along the limit cycle and the resulting trajectory corresponding to this perturbation is along the same limit cycle.

One curious thing happens for slightly larger slopes. There is a bifurcation of the solution and the robot

exhibits a limit cycle which repeats itself every *two* cycles. Physically, this means that two successive steps of the robot are not identical. A local stability analysis (see Section 5) shows that the gait is stable.

6 An energy tracking control law

Here we introduce a simple control law which was inspired by the passive energy characteristics of the compass model. Please recall that when the robot walks down the slope its pivot point also shifts downward at every touchdown. As it loses gravitational PE in this way it is expected that its kinetic energy should increase accordingly. This is exactly the amount of energy that is to be absorbed by the impact. If, at every touchdown we bring down our PE reference line to the point of touchdown, the total energy of the robot appears constant regardless of its downward motion. This is the principle we apply to formulate a control strategy for the robot. The control law, aware of the characteristic energy of the natural limit cycle for the given slope, tries to drive the robot to that energy level.

The total energy E of the robot can be expressed as $E = 0.5\dot{\boldsymbol{\theta}}^T \boldsymbol{M}\dot{\boldsymbol{\theta}} + PE$. The power input to the system is the time rate of change of total energy, $\dot{E} = \dot{\boldsymbol{\theta}}^T \boldsymbol{S}\boldsymbol{u}$ where $\boldsymbol{u}$ is the actuator torque vector and $\boldsymbol{S}$ is the selection matrix. For a passive cycle, $\boldsymbol{u} = 0$ and the associated energy $E^* = E(\dot{\boldsymbol{\theta}}^*, \boldsymbol{\theta}^*)$. Suppose now that we use a simple damper control law of the form $\boldsymbol{S}\boldsymbol{u} = -\beta\dot{\boldsymbol{\theta}}$. The power input to the system is therefore $\dot{E} = -\dot{\boldsymbol{\theta}}^T \beta\dot{\boldsymbol{\theta}}$. For a positive definite β, the quantity $-\dot{\boldsymbol{\theta}}^T \beta\dot{\boldsymbol{\theta}} < 0$.

Let us specify that our control law should attempt to bring the current energy level of the robot to the target energy level at an exponential rate. Also assume that we use only the actuator input at the hip joint of the robot. A control law of the following form will achieve this:

$$\dot{E} = -\lambda(E - E^*) = \dot{\boldsymbol{\theta}}^T \boldsymbol{S}\boldsymbol{u} = \begin{bmatrix} \dot{\theta}_{ns} & \dot{\theta}_s \end{bmatrix} \begin{bmatrix} -u_H \\ u_H \end{bmatrix} \qquad (10)$$

from which we can calculate

$$u_H = \frac{-\lambda(E - E^*)}{\dot{\theta}_s - \dot{\theta}_{ns}} \qquad (11)$$

While implementing this law we only need to be cautious when $\dot{\theta}_s - \dot{\theta}_{ns} = 0$.

In Figure 4 we show an "active" cycle superimposed on the passive cycle on a 3° slope. The advantage of the active control becomes clear when we note that the starting position shown in the figure lies outside the basin of attraction of the passive limit cycle. In other words the passive robot will fall down soon if it starts from this initial condition. The effect of the active control law is therefore to expand the basin of attraction of the passive limit cycle. Besides, we have found that non-natural cycles can be realized by using 2 actuators by specifying a suitable E^* [5].

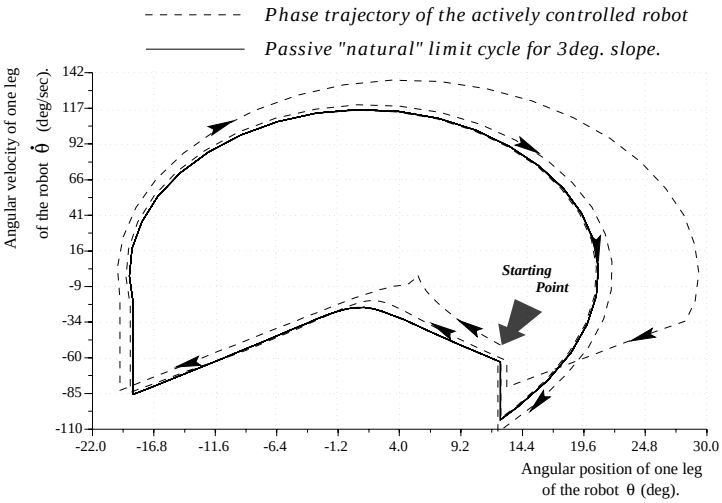

Figure 4: Active stabilization of a limit cycle. Here we show the performance of the energy tracking control law for a robot walking down on a 3° slope. The system driven only by a hip torque seeks and returns to the passive cycle of the robot. The initial conditions from which the system is brought to the limit cycle lie outside the basin of attraction of the passive limit cycle.

7 Conclusions and future work

We have studied the stability and the periodicity properties of the passive motion of a simple biped machine, the compass gait walker. We have shown that such a biped can walk down an inclined plane in a steady periodic fashion. There is a strong indication that all the motion descriptors of such a gait are determined by only one parameter, the slope of the inclined plane. The motion equations exhibit a bifurcation phenomenon at a certain slope angle when a symmetric periodic motion changes to another stable periodic motion with unequal step lengths.

We have introduced a simple control law in the spirit of the passive characteristics of such a motion and demonstrated that the basin of attraction of the limit cycle can be significantly enlarged by the introduction of one control input.

Although not useful as a viable "walk", the unstable limit cycles in our system may tell us more about

its global properties. In order to identify the unstable limit cycles we would need to integrate the system back in time. We should remember that our system's behavior is heavily influenced by our impact model which is not by any means the only available impact model. It will be useful to be able to identify the boundary of the basin of attraction and to determine the favorable initial conditions. In order for a control law to be robust and reliable, the limit cycle associated with it should have a reasonably wide basin of attraction.

Our present study is a precursor of our exploration of a simple biologically inspired control law for a multi DOF anthropomorphic biped robot prototype.

References

[1] Bavarian, B.; Wyman, B.F.; Hemami, H., 1983 Control of the Constrained Planar Simple Inverted Pendulum. *International Journal of Control, Vol. 37, No. 4, pp.344-358*

[2] Berkemeier, M.D., Fearing, R.S. 1992 Control of a Two-Link Robot to Achieve Sliding and Hopping Gaits. *Proc. of IEEE Conf. on Robotics and Automation, Nice, Vol. 1, pp.286-291*

[3] Block, D.J., Spong, M.W. 1995 Mechanical Design & Control of the Pendubot. *SAE Earthmoving Industry Conference, Peoria, IL*

[4] Golliday, C.L., H. Hemami, 1977. An Approach To Analyzing Biped Locomotion Dynamics and Designing Robot Locomotion Controls. *IEEE Transactions on Automatic Control AC 22(6), pp. 963-972*

[5] Goswami, A., B. Espiau, A. Keramane, F. Genot 1995. The gait of a compass-like biped robot: limit cycles, passive stability, and active control *Internal Report, INRIA, (to appear)*

[6] Guckenheimer, J., P. Holmes, 1983. Nonlinear Oscillations, Dynamical Systems, and Bifurcations. *Springer-Verlag, New York*

[7] Hayashi, C. 1985 Nonlinear Oscillations in Physical Systems. *Princeton Univ Press, NJ*

[8] Hurmuzlu, Y. ; Chang, T.-H. 1992. Rigid Body Collisions of a Special Class of Planar Kinematic Chains. *IEEE Transactions on SMC, Vol. 22, No. 5, pp.964–971*

[9] Katoh, R., M. Mori, 1984. Control Method of Biped Locomotion Giving Asymptotic Stability of Trajectory. *Automatica, Vol.20, No.4, pp.405-411*

[10] Kelso, J.A.S., Holt, K.G., Rubin, P., Kugler, P.N. 1981. Patterns of Human Interlimb Coordination Emerge from the Properties of Non-Linear, Limit Cycle Oscillatory Processes: Theory and Data. *Journal of Motor Behavior, Vol.13, No.4, pp.226-261*

[11] McGeer, T. 1990 Passive Dynamic Walking. *International Journal of Robotics Research, 9-2, pp. 62-82*

[12] Miura, H., I. Shimoyama, 1984. Dynamic Walk of a Biped. *International Journal of Robotics Research, 3-2, pp. 60-74*

[13] Ott, E. 1993 Chaos in Dynamical Systems. *Cambridge University Press, UK*

[14] Spong, M. W. 1995. The Swing Up Control Problem for the Acrobot. *IEEE Control Systems Magazine, February*